Journal of Geosciences, 57 (2012), 53–62 DOI: 10.3190/jgeosci.111

Original paper

Raman spectra of minerals containing interconnected As(Sb)O_3 pyramids: trippkeite and schafarzikite

Sherif KHARBISH

Geology Department, Faculty of Science, Suez Canal University, Suez Branch, Suez Governate, El Salam City, 44634, Egypt; sherifkharbish@hotmail.com, Sherif_abdallah@s-science.suez.edu.eg

Oriented single-crystals of trippkeite ($CuAs_2O_4$) and an isostructural mineral schafarzikite ($FeSb_2O_4$) were investigated by polarized Raman spectroscopy. The internal vibrations, i.e. the stretching and bending modes, of trippkeite occur between 250 and 850 cm^{-1}, and those of schafarzikite between 200 and 750 cm^{-1}. The higher mass and the longer bond distances of the SbO_3 groups readily explain the lower wavenumbers of the latter. Comparing the spectra of minerals containing XO_3 pyramids with those of the minerals from the present study, approximate similarities in the spectral features are evident. A clear distinction between Raman spectra of separated and interconnected (As,Sb)O_3 groups is not observed.

Keywords: oriented single-crystals, pyramidal (As,Sb)O_3 groups, Raman spectroscopy, schafarzikite, trippkeite
Received: 7 December 2011; accepted: 8 March 2012; handling editor: J. Sejkora

1. Introduction

Trippkeite ($CuAs_2O_4$) and an isostructural schafarzikite ($FeSb_2O_4$) are relatively rare in nature. Both minerals belong to the group of compounds with a general formula AB_2O_4, where A represents a divalent metal ion such as Pb, Cu, Sn, Ni, Zn, Mn, Fe and/or Mg, whereas the B represents trivalent metal ions like Pb, As, Sb Al, Cr and/or Mg (Hinrichsen et al. 2006). The trippkeite possesses AsO_3 chain polymer (Lee and Harrison 2004), which was first definitively characterized by Zemann (1951b). Pertlik (1988) also showed that the two synthetic lead chain-arsenite chlorides $Pb(AsO_2)Cl$ and $Pb_2(AsO_2)_3Cl$ contain the same AsO_3 chain polymer, as does the mineral leiteite, $ZnAs_2O_4$ (Ghose et al. 1987). Schafarzikite is a meta-antimonite mineral containing polymeric SbO_3 pyramids (Krenner 1921; Zemann 1951a; Fischer and Pertlik 1975; Sejkora et al. 2007). Despite the work that has been done on the crystal structures of trippkeite and schafarzikite, Raman spectroscopic studies, at least of oriented trippkeite, have not been published so far. In general, there exist very few works dealing with Raman spectroscopy of "not oriented" trippkeite (Bahfenne 2011; Bahfenne et al. 2011) or "not oriented" (Sejkora et al. 2007) and "oriented" schafarzikite (Bahfenne 2011; Bahfenne et al. 2011).

The purpose of the present work is therefore (1) to investigate oriented crystals of synthetic trippkeite and naturally occurring schafarzikite by Raman spectroscopy, (2) to examine the spectral changes related to crystal structural features, such as bond distances and (As,Sb)O_3 groups of reduced (non-trigonal) symmetry (all minerals of the present study) vs. isolated pyramidal (As,Sb)O_3 groups of ideal trigonal symmetry.

2. Crystallographic data

Trippkeite ($CuAs_2O_4$) and schafarzikite ($FeSb_2O_4$) crystallize in space group $P4_2/mbc$ (D_{4h}^{13}) with four formula units per unit cell (Z = 4). The structure of trippkeite was first solved by Zemann (1951b) and was refined by Pertlik (1975). Eby and Hawthorne (1993) mentioned that trippkeite has rutile-like chains. The trippkeite crystal structure is illustrated in Fig. 1a. There are two kinds of O atoms, O(1) and O(2). The Cu atoms are surrounded octahedrally by six O atoms [four O(2) and two O(1)] (Pertlik 1975). The As atoms are coordinated by three O atoms [two O(1) and one O(2)] to form a flat trigonal pyramid (Fig. 1a) (Zemann 1951b; Pertlik 1975). The As–O(1) and As–O(2) interatomic distances in trippkeite are 1.814 (2x) and 1.765 Å, respectively (Pertlik 1975). The O(1)–As–O(2) and the O(1)–As–O(1) angles are 95.9° (2x) and 100.3°, respectively (Pertlik 1975). The As polyhedra are connected by common corners, building chains parallel to the *c*-axis, into which the lone pairs of the As^{3+} point (Pertlik 1975; Eby and Hawthorne 1993).

The structure of schafarzikite, containing small amounts of Mn^{2+}, has been determined by Zemann (1951a) and refined by Fischer and Pertlik (1975). The crystal structure of schafarzikite is built up by columns, running along (001), of edge-sharing Fe^{2+} octahedra; parallel to these are chains of corner-sharing Sb^{3+}

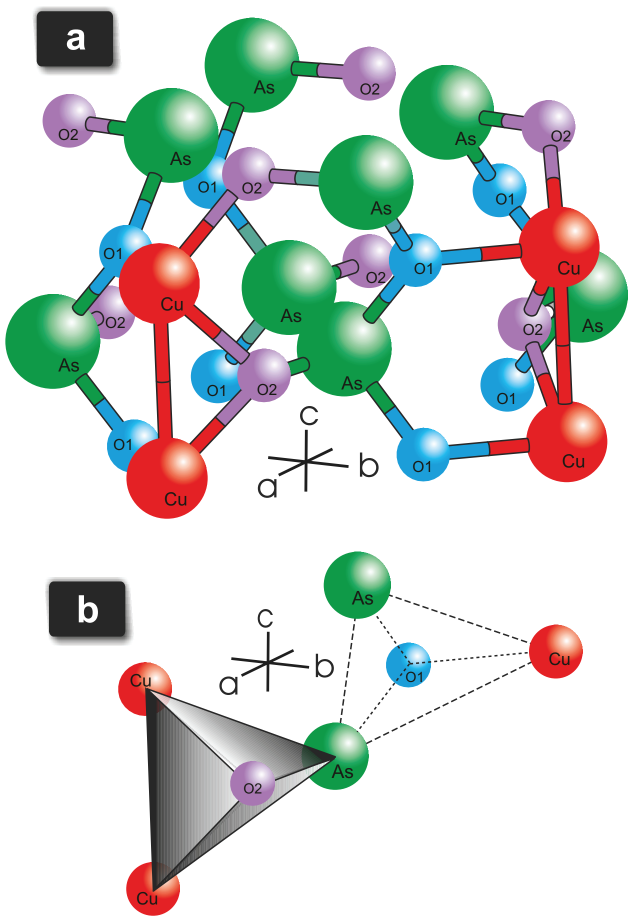

Fig. 1 Crystal structure of trippkeite redrawn after Pertlik (1975) (**a**), and the interconnection of the oxygen atoms to the surrounding ones (**b**).

ψ-tetrahedra (Mellini and Merlino 1979), namely trigonal pyramids with a lone pair as fourth ligand (Cotton and Wilkinson 1966). All the O atoms of each tetrahedral chain lie on one plane, parallel to (110); successive Sb atoms of the chain are located on opposite sides of this plane (Fischer and Pertlik 1975). The connection between chains and octahedral columns builds up a framework with open channels parallel to (001) (Mellini and Merlino 1979). The diameter of the channels is related to the distance (4.1 Å) between antimony atoms lying on opposite sides of the channels and pointing their lone pairs one toward the other (Mellini and Merlino 1979). Similar to the trippkeite, each Sb in schafarzikite is connected to two O(1) and one O(2) and each Fe is connected to four O(2) and two O(1). The Sb–O(1) and Sb–O(2) interatomic distances in schafarzikite are 1.987 (2x) and 1.917 Å, respectively, whereas the O(1)–Sb–O(2) and O(1)–Sb–O(2) angles, 93.5° (2x) and 96.0°, respectively (Fischer and Pertlik 1975).

Inspection of the crystal structure of the trippkeite and schafarzikite reveals two kinds of O atoms [i.e. O(1) and O(2)]. O(1) atom is bonded to two As(Sb) and one Cu(Fe) atoms, forming a planar triangular group (Fig. 1b), whereas O(2) atom is connected to two Cu(Fe) and one As(Sb) atoms, forming a pyramidal group (Fig. 1b) (Fischer and Pertlik 1975; Pertlik 1975). Therefore, the $As(Sb)O_3$ pyramids in trippkeite and schafarzikite should be considered as interconnected group (i.e. all the O atoms are bridging atoms). However, in synthetic oxo-antimonates and -arsenates, the O atoms with longer interatomic distances are considered as bridging and those with shorter interatomic distances as terminal atoms (Hirschle and Röhr 2000; Emmerling and Röhr 2003).

3. Samples and experimental

Raman spectroscopic measurements were done on synthetic trippkeite and naturally occurring schafarzikite samples. The synthetic trippkeite samples were kindly provided by Prof. Pertlik, Vienna. The natural schafarzikite samples (Pernek, Slovakia) are from the collection of the Institute of Mineralogy and Crystallography, University of Vienna. The trippkeite and schafarzikite samples are part of the original material that has been used for the crystal structure refinement by Zemann (1951a, b), Fischer and Pertlik (1975) and Pertlik (1975).

The unit-cell parameters of the trippkeite and schafarzikite were determined on a single-crystal X-ray Nonius Kappa four-circle diffractometer, equipped with a CCD detector and a 300 µm capillary optics collimator. Data were acquired using the program Collect, processed with the Nonius software suite DENZO-SMN (Otwinowski and Minor 1997) and corrected for Lorentz, polarization and background effects. The full-matrix least-squares refinement was undertaken using the program SHELXTL 6.12 (Bruker Analytical X-ray Solutions), using neutral-atom scattering factors and corrections for anomalous dispersion. No change in the reflections was noticed.

Carefully separated single grains of trippkeite and schafarzikite were (i) oriented according to morphology, and then (ii) mounted on glass rods and oriented by using a Nonius Kappa CCD diffractometer.

The chemical compositions of trippkeite and schafarzikite samples were measured on a Jeol JSM-6400 scanning electron microscope equipped with a Link EDX unit. Cobalt was used for internal gain calibration. An acceleration voltage of 20 kV was applied, the channel width was set to 20 eV, matrix absorption and fluorescence effects were corrected for by the ZAF-4 algorithm (Link Analytical). The analyses were accurate to 1 %.

Raman spectra were collected with the laser polarization parallel to the *a*- and *c*-axes for the tetragonal trippkeite and schafarzikite minerals. The spectra of all minerals were acquired in the spectral range from 50 to 1200 cm^{-1} by using a Renishaw RM1000 confocal notch filter-based micro-Raman system. The 785 nm excitation line of a 17 mW solid-state laser (attenuated to 4.25 mW for schafarzikite) with polarization extinction > 500:1 was focused with a 50× /0.75 objective on the sample surface. The laser polarization was parallel to the a- and c-axes. The back-scattered radiation (180° configuration) was analyzed with a 1200 lines/mm grating monochromator in the so-called "static grating scan" data collection mode. Raman intensities were collected with a thermo-electrically cooled CCD array detector. The resolution of the system ("apparatus function") was 2 cm^{-1} and the wavenumber accuracy was ± 1 cm^{-1} (both calibrated with the Rayleigh line and the 520.5 cm^{-1} line of a Si standard). Instrument control and data acquisition were done with Grams/32 software (Galactic Ind. Corp.). Depending on the signal intensity, accumulations with 60–120 s for trippkeite and 60–90 s for schafarzikite per "spectral window" (i.e., exposure time of the detector) were measured. The peak centers of single bands were determined by fits of combined Gaussian/Lorentzian amplitude functions using the PeakFit 4.12 software (Jandel Scientific).

4. Results

4.1. Sample characterizations

Trippkeite crystals are short prismatic to equant in shape and greenish blue in color (pale bluish green in transmitted light); they show a vitreous luster. The unit-cell parameters for trippkeite are a = 8.5941(3) and c = 5.5728(4) Å. Schafarzikite crystals are prismatic, dark brown to black in color and have an adamantine to metallic luster with unit-cell parameters a = 8.6012(3) and c = 5.9133(4) Å. The newly refined unit-cell dimensions are in an excellent agreement with those given by Pertlik (1975) for trippkeite (a = 8.59 and c = 5.57 Å) as well as by Fischer and Pertlik (1975) and Sejkora et al. (2007) for schafarzikite (a = 8.59 and c = 5.91 Å). The structural formulae calculated from the chemical analyses on the basis of four oxygen atoms per formula unit are $Cu_{1}.05As_{1.95}O_4$ (trippkeite) and $(Fe_{0\cdot 9}Mn_{0.1})Sb_{2.0}O_4$ (schafarzikite).

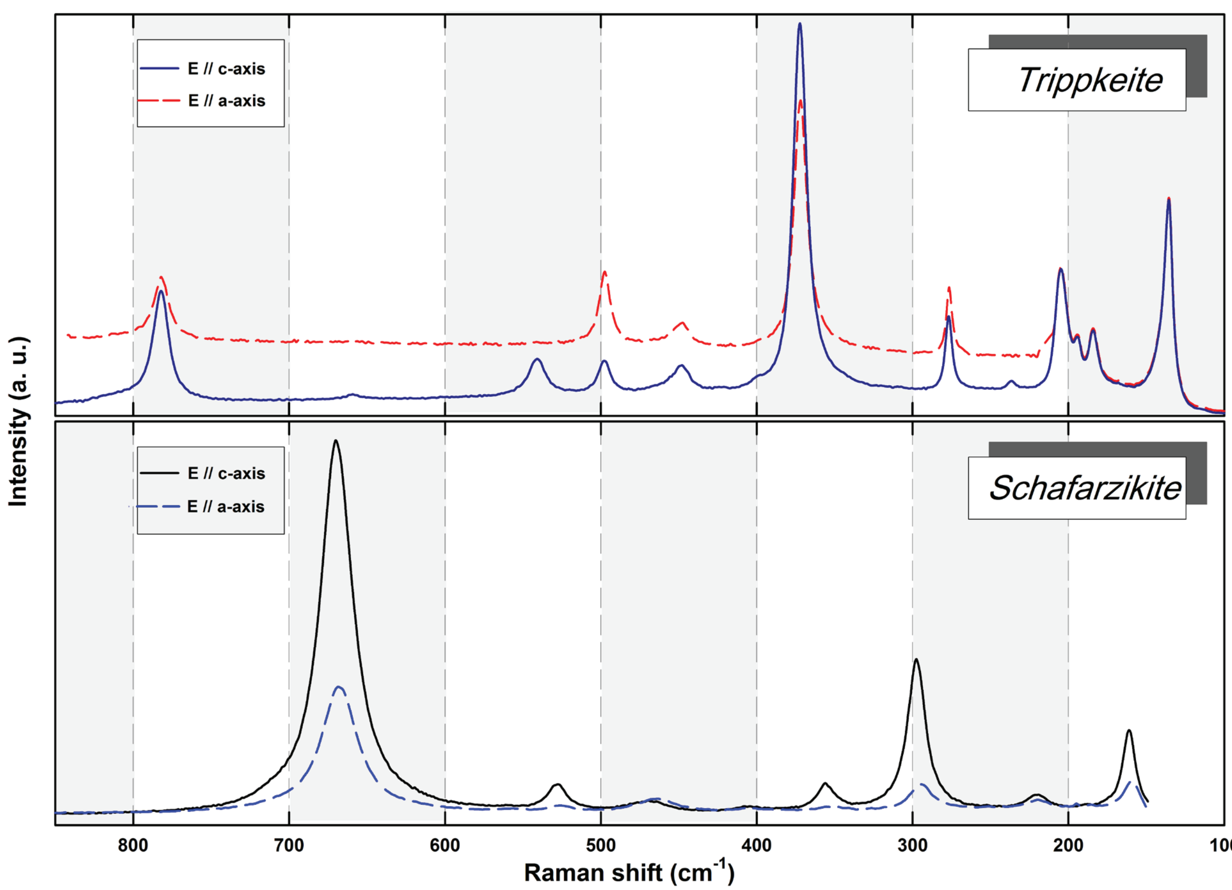

Fig. 2 Raman spectra and vibration modes of trippkeite and schafarzikite. E // c- axis, solid line; E // a-axis, dashed line.

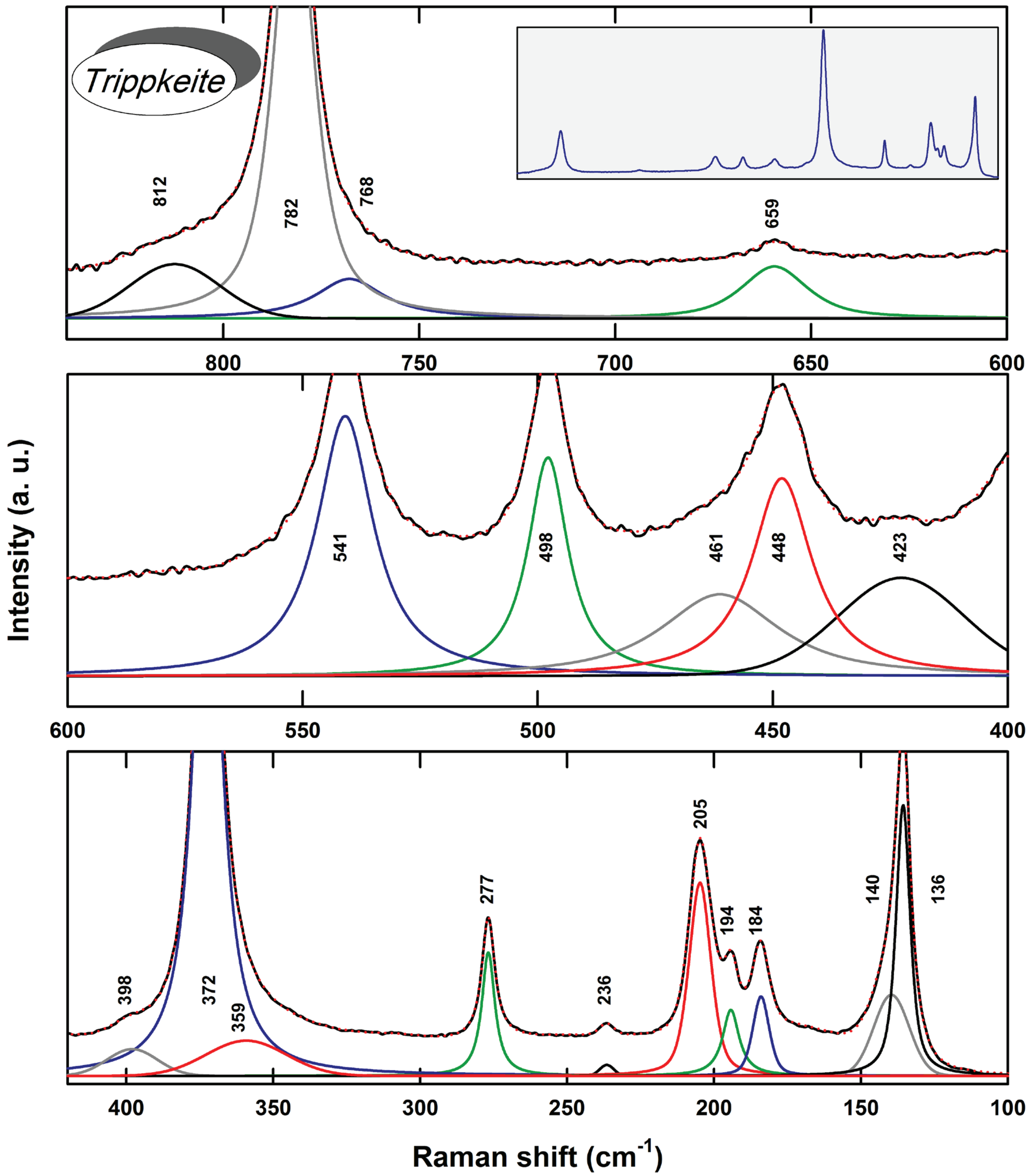

Fig. 3 The positions of the bands (cm^{-1}) of trippkeite obtained by using the PeakFit program. Goodness of fit (r^2) > 0.998.

4.2. Raman spectra of trippkeite

The bands in the trippkeite spectra parallel to the *a*- and *c*-axes occur in the vibrational region between 100 and 850 cm^{-1} (Fig. 2). No additional bands were observed in lower or higher wavenumber regions. There is nearly no difference in the band numbers and positions between the trippkeite spectra obtained parallel to the *a*- and *c*-axes (Fig. 2). However, the band intensities measured parallel to the *c*-axis are significantly greater than those measured parallel to the *a*-axis. Raman spectra are characterized by a very strong band at 372 cm^{-1} and strong band at 782 cm^{-1}. In the spectra of trippkeite (parallel to the *a*- and *c*-axes), four vibration regions can be also easily distinguished (Fig. 2). The first occurs between 850 and 600 cm^{-1}. Peak fitting reveals four medium, weak to very weak bands at 812, 782, 768 and 659 cm^{-1} (Fig. 3). Five weak, medium to very strong bands and shoulders at 541, 498, 461, 448 and 423 cm^{-1} are noticed in the second region (i.e. between 600 and 400 cm^{-1}). The fitting of the third region between 400 and 250 cm^{-1} reveals four very strong, medium to very weak vibrational modes at 398, 372, 359 and 277 cm^{-1}. The last region appears below 250 cm^{-1}.

4.3. Raman spectra of schafarzikite

The spectra of schafarzikite were also collected parallel to the *a*- and *c*-axes (Fig. 2). The bands occur in the vibrational region between 150 and 750 cm^{-1} (Fig. 2). The band numbers and positions measured parallel to the *a*- and *c*-axes are identical. Similar to the case of trippkeite, the intensities of the bands measured parallel to the *c*-axis are also significantly greater than those observed perpendicular to the *c*-axis. The spectra of schafarzikite are characterized by a very intense band at 668 cm^{-1} and strong band at 295 cm^{-1}. In the spectra measured in both directions, four vibration regions can be easily observed (Fig. 2). The first region, between 750 and 500 cm^{-1}, contains a very strong sharp band at 668 cm^{-1} and weak bands and/or shoulders at 707, 555 and 526 cm^{-1} (Fig. 4). The second region occurs between 500 and 300 cm^{-1}. Band fitting reveals four medium, weak to very weak bands at 464, 405, 353 and 347 cm^{-1}. The third region (300–200 cm^{-1}) contains five medium to very weak modes at 295, 275, 253, 229 and 218 cm^{-1}. The last region (< 200 cm^{-1}) contains four medium to very weak modes.

5. Discussion and conclusions

Raman bands of trippkeite as well as of schafarzikite samples were observed between 100 and 850 cm^{-1} (Fig. 2, Tab. 1), with the low-energy limit determined only by the cut-off value of the employed Raman notch and edge filters. No additional bands were observed in lower or higher wave number regions. The band positions of both minerals agree with the characteristic spectral regions of oxides (700–300 cm^{-1}) (Wang et al. 1994).

According to the "harmonic oscillator model" and Hooke's law, the frequency of vibrational modes in isostructural phases is shifted with the substitution of one element by another (or even one isotope by another). Thus, bands move to higher wave numbers with increasing bond strength (e.g. shorter bond lengths) and reduced mass.

The shift of the vibrational regions between trippkeite and schafarzikite (Fig. 2) is attributed to the difference in the atomic masses between As and Sb, which simply explains the appearance of the trippkeite vibrational bands at wave numbers higher than in case of schafarzikite. On the other hand, band shifts can be related to differences in bonding behavior and, most evidently, to different bond lengths. Thus, the shorter As–O bonds in trippkeite (1.814 (2x), 1.765Å; as recorded by Pertlik 1975) should result in vibrational modes at higher wave numbers than the longer Sb–O bonds in schafarzikite (1.987 (2x), 1.917Å; as recorded by Fischer and Pertlik 1975).

Inspection of the spectra of the two studied minerals (Fig. 2) reveals that the band numbers and positions are not affected by the polarization directions of the incident laser beam. However, the band intensities are affected considerably and maximum intensities are observed parallel to the *c*-axis (Fig. 2). An apparent reason for this behavior is that the band intensities depend on the direction of the molecular axes of the $(AsSb)O_3$ pyramids, which are all aligned parallel to the c-axis, pointing only in one direction. In other words, the c-direction provides the strongest change in polarizability, i.e. the strongest component of the Raman tensor.

The trippkeite and schafarzikite minerals should exhibit the characteristic vibrational modes of $(As,Sb)O_3$ groups and further lattice modes of the mineral constituents. According to Loehr and Plane (1968) and Nakamoto (1997), an isolated ideal pyramidal $(As,Sb)O_3$ group, which belongs to the C_{3v} point group, is expected to show only four normal modes of vibration (i.e. $2A_1 + 2E$). All four modes of vibration of a pyramidal $(As,Sb)O_3$ group are IR- and Raman active (Nakamoto 1997). The symmetric (As,Sb)–O stretching mode is expected to lie at a higher frequency than the asymmetric mode (Loehr and Plane 1968). The two stretching frequencies symmetric ν_1 (A_1) and antisymmetric ν_3 (E), as well as the two bending frequencies, symmetric ν_2 (A_1) and antisymmetric ν_4 (E), overlap or are close in energy in most of similar compounds showing a sequence in wave number, i.e. $\nu_1 > \nu_3 > \nu_2 > \nu_4$ (Nakamoto 1997).

Although only four normal modes of vibration (i.e. $2A_1 + 2E$) should occur in the spectra of trippkeite and schafarzikite according to Loehr and Plane (1968) and Nakamoto (1997), both minerals show additional bands. The question why the number of bands increases can be explained if it is considered to be a function of the symmetry of the $(As,Sb)O_3$ pyramids. In the investigated minerals the symmetry of the pyramidal $(As,Sb)O_3$ groups is reduced to C_s. On a C_s symmetry A_1 modes translate into A' and E modes split to A' and A" (Nakamoto 1997; Bahfenne et al. 2011). Correlating this to a D_{4h} crystal system splits each A' mode to A_{1g}, A_{2g}, B_{1g}, B_{2g} and $2E_u$ and each A" mode to A_{1u}, A_{2u}, B_{1u}, B_{2u} and

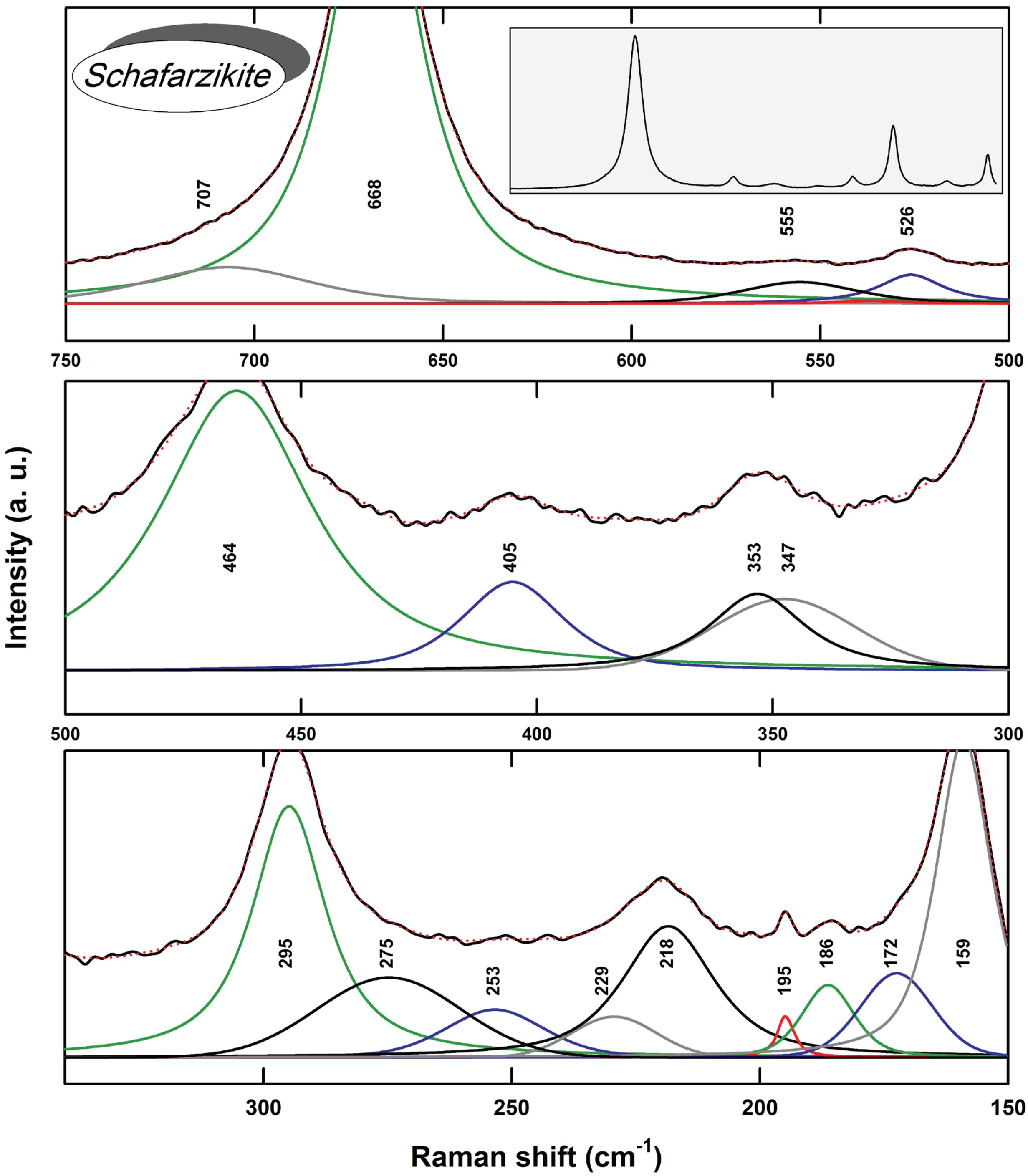

Fig. 4 The positions of the bands (cm^{-1}) of schafarzikite obtained by using the PeakFit program. Goodness of fit (r^2) > 0.997

$2E_g$. Only the g vibrational modes (i.e. A_{1g}, B_{1g}, B_{2g} and $2E_g$) are Raman active, whereas the u modes are either inactive or IR active (Fig. 5 shows the splitting pattern of the A_1 and E modes).

Band assignments (Tab. 1) are based on the sequence of band energies given by Nakamoto (1997) with $\nu_1 > \nu_3 > \nu_2 > \nu_4$ and are also facilitated by comparing the band positions with those given by Bahfenne (2011), Bahfenne et al. (2011) and Sejkora et al. (2007) for trippkeite and schafarzikite and those presented by Hirschle and Röhr (2000) and Emmerling and Röhr (2003) for oxo-arsenates and -antimonates.

Tab. 1 Band assignment, band positions (cm^{-1}) and FWHM for the Raman spectra of trippkeite and schafarzikite in comparison with literature data

		trippkeite					schafarzikite					
		Symmetry	Band cm^{-1}	FWHM	Band cm^{-1}		Symmetry	Band cm^{-1}	FWHM	Band cm^{-1}		
		Present study			T[1]	T[2]	Present study			**S[1]**	**S[2]**	**S[3]**
As(Sb)–O		A_{1g}	812vw	25.05	810	810	A_{1g}	707vw$_s$	51.65	709	708	
symmetric stret-	ν_1	A_{2g}	782s	11.95	780	780	A_{2g}	668vs	27.87	668	667	670
ching		B_{1g}	768vw$_s$	21.00						617	616	617
As(Sb)–O												
antisymmetric	ν_3						A_{1g}	555vw	36.20	558	557	
stretching		A_{1g}	659w	20.06	657	657	A_{2g}	526w	20.86	526	525	524
		A_{1g}	541m	14.47	539	539				478		
As(Sb)–O–(Sb)		A_{2g}	498m	10.32	496	496	A_{1g}	464m	38.20	465	465	467
As symmetric	ν_2	B_{1g}	461vw$_s$	29.95			A_{2g}	405w	25.63	403	402	405
bending		B_{2g}	448w	15.46			B_{1g}	353w	24.40	353	352	
		?	423vw	30.09	421	421	B_{2g}	347vw	39.98	345	344	348
		A_{1g}	398vw	20.30			A_{1g}	295m	17.81	295	295	295
As(Sb)–O–(Sb)		A_{2g}	372vs	10.73			A_{2g}	275w$_s$	34.10			
As antisymmetric	ν_4	B_{1g}	359vw	32.21	371	371	B_{1g}	253vw	23.60	249	249	
bending		B_{2g}	227s	5.38			B_{2g}	229w	19.99			
							E_g	218w	21.99	219	219	217
										208	208	
			236vw	5.69								
			205s	8.86						186	186	
			194m	6.38				195w	3.99			
Lattice modes			184m	3.66				186w	12.44	158	159	
			140vw$_s$	12.20				172w$_s$	17.12	132	131	
			136s	5.70				159m	13.26	119	119	
										107	107	

vs = very strong, s = strong, m = medium, w = weak, vw = very weak, w$_s$ = weak shoulder, vw$_s$ = very weak shoulder (average relative band intensities from all polarization directions).
T[1] trippkeite data and S[1] schafarzikite data after Bahfenne (2011)
T[2] trippkeite data and S[2] schafarzikite data after Bahfenne et al. (2011)
S[3] schafarzikite data after Sejkora et al. (2007)

In trippkeite (Figs 2–3) the strong band at 782 cm^{-1} and two very low intensity shoulders at 812 and 768 cm^{-1} were assigned to the symmetric ν_1 (A_1) As–O stretching modes (Tab. 1). This band triplet was also assigned to A_{2g}, A_{1g} and B_{1g}, respectively (Tab. 1). The very weak band at 659 cm^{-1} was assigned to the antisymmetric ν_3 (E) stretching mode and also to A_{1g} (Tab. 1). The modes at 812, 782 and 659 cm^{-1} were ascribed previously to stretching vibrations by Bahfenne (2011) and Bahfenne et al. (2011). The mode at 768 cm^{-1} has never been recorded in trippkeite previously.

The medium and low intensity bands and shoulders at 541 (A_{1g}), 498 (A_{2g}), 461 (B_{1g}), 448 (B_{2g}) and 423(?) cm^{-1} in trippkeite were assigned to the symmetric ν_2 (A_1) bending modes, whereas the very intense band and the strong band at 372 (A_2g) and 277 (B_2g) cm^{-1}, respectively, as well as the very weak shoulders at 398 (A_{1g}) and 359 (B_{1g}) cm^{-1}, ascribed to the antisymmetric ν_4 (E) bending modes (Figs 2–3; Tab. 1).

Although the bands at 541, 498, 423 and 372 cm^{-1} were recorded by Bahfenne (2011) and Bahfenne et al. (2011), only the latter two had been assigned to bending vibrations. The bands at 541 and 498 cm^{-1} were considered as Cu–O stretching vibrations by Bahfenne et al. (2011) or as As–O stretching vibrations by Bahfenne (2011).

In trippkeite, absorption bands which are not related to stretching or bending modes of AsO_3 groups occur below ~ 250 cm^{-1} (Tab. 1). The other bending and all lattice modes have never been reported in trippkeite previously, either.

The symmetric ν_1 (A_1) Sb–O stretching modes in schafarzikite consist of the very strong dominant Raman band at 668 (A_{2g}) cm^{-1} and the very weak shoulder at 707 (A_{1g}) cm^{-1} (Figs 2, 4; Tab. 1). The antisymmetric ν_3 (E) Sb–O stretching vibrations occur as weak to very weak bands at 555 (A_{1g}) and 526 (A_{2g}) cm^{-1} (Figs 2, 4; Tab. 1). The weak to very weak band triplet at 464 (A_{1g}), 405 (A_{2g}) and 353 (B_{1g}) cm^{-1} with the weak satellite shoulder at 347 (B_{2g}) cm^{-1} were considered as the symmetric ν_2 (A_1) bending modes (Figs 2, 4; Tab. 1). The strong and medium bands at 295 (A_{1g}) and 218 (E_g) as well as the weak shoulders at 275 (A_{2g}), 253 (B_{1g}) and 229 (B_{2g}) cm^{-1} were assigned to the antisymmetric ν_4 (E) bending modes. The bands occurring below ~ 200 cm^{-1} are ascribed to lattice vibrational modes (Figs 2, 4; Tab. 1). The bands at 275, 229 cm^{-1} and some lattice mode have never been recorded in schafarzikite spectrum previously. The other modes had

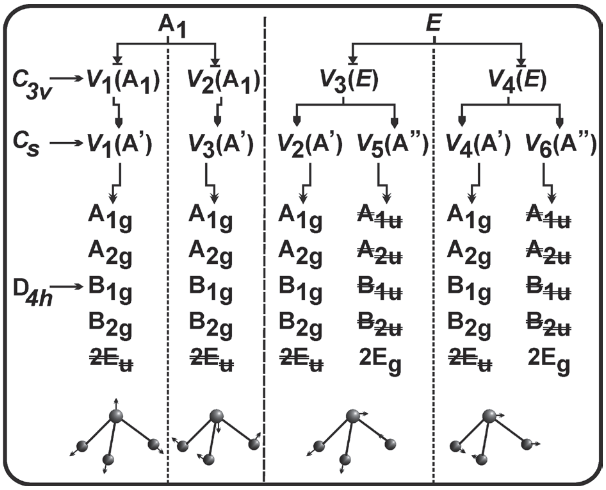

Fig. 5 Splitting pattern of the A_1 and E modes. (Modes with strikethrough are either IR active or inactive).

been reported by Sejkora et al. (2007), Bahfenne (2011) and Bahfenne et al. (2011).

Comparison of the band positions and numbers of the present study with those given by Sejkora et al. (2007), Bahfenne (2011) and Bahfenne et al. (2011) shows a great similarity in the band positions and an increase in the band numbers, especially in the spectrum of trippkeite (Tab. 1). The increase in the bands numbers in trippkeite spectra may be attributed to the oriented measurements. Bahfenne et al. (2011) expected that other bands should be occurring in the spectra of trippkeite and schafarzikite.

In the present work, the assignment of some bands (Tab. 1) differs from that given by Bahfenne et al. (2011). Thus the bands at 541 and 498 cm^{-1} in trippkeite and at 464 and 405 cm^{-1} in schafarzikite were assigned to Cu(Fe)–O stretch and the bands at 238 and 218 cm^{-1} in schafarzikite to Fe–O deformation by Bahfenne et al. (2011). However, there was presented no evidence to support such a symmetry assignment. Furthermore, Bahfenne (2011) ascribed the same bands (i.e. 541 and 498 cm^{-1} in trippkeite and 464 cm^{-1} in schafarzikite) to As(Sb)–O stretching vibrations. Moreover, comparing the spectra of trippkeite with those of arsenolite and claudetite, unsurprisingly, the spectra of latter minerals show the same bands at 536 cm^{-1} (arsenolite, Gilliam et al. 2003), 541 cm^{-1} (claudetite, Flynn et al. 1976) and 504 cm^{-1} (claudetite, Origlieri et al. 2009).

In addition, Loehr and Plane (1968) and Flynn et al. (1976) have collected the spectra of isolated C_{3v} pyramidal AsO_3 group and assigned the bands between ~ 750 and 300 cm^{-1} to the vibrational modes of the isolated AsO_3 pyramids. The bands between ~ 850 and 250 cm^{-1} were assigned also to the vibrational modes of the interconnected (C_s) pyramidal AsO_3 group in claudetite (As_2O_3) (Flynn et al. 1976; Origlieri et al. 2009), arsenolite (As_2O_3) (Beattie et al. 1970; Brumbach and Rosenblatt 1972; Lucovsky and Galeener 1980; Grzechnik 1999; Gilliam et al. 2003; Jensen et al. 2003), leiteite ($ZnAs_2O_4$) and stibioclaudetite ($AsSbO_3$) (Origlieri et al. 2009), oxo-arsenates (Emmerling and Röhr 2003) and oxo-antimonates (Hirschle and Röhr 2000).

Comparison of band positions of the isolated C_{3v} and interconnected C_s pyramidal XO_3 group (Figs 6–7) shows that the stretching and bending vibrations of the isolated and interconnected AsO_3 and interconnected SbO_3 pyramids occur in the spectral region between 850–250 and 750–200 ± 20 cm^{-1}, respectively, which is considered the characteristic spectral region of oxides (according to Wang et al. 1994). The vibrational modes that appear below 250 ± 20 and below 200 ± 20 cm^{-1} can be attributed to the lattice vibrational modes of AsO_3 and SbO_3 pyramids, respectively. According to the former observation, it can be speculated that the vibrational modes of the As(Sb)O_3 pyramids (isolated and interconnected) should appear in this spectral region (namely, between 850 and 200 ± 20 cm^{-1}) (Figs 6–7). Accordingly, the bands occurring between 540 and 450 cm^{-1} in

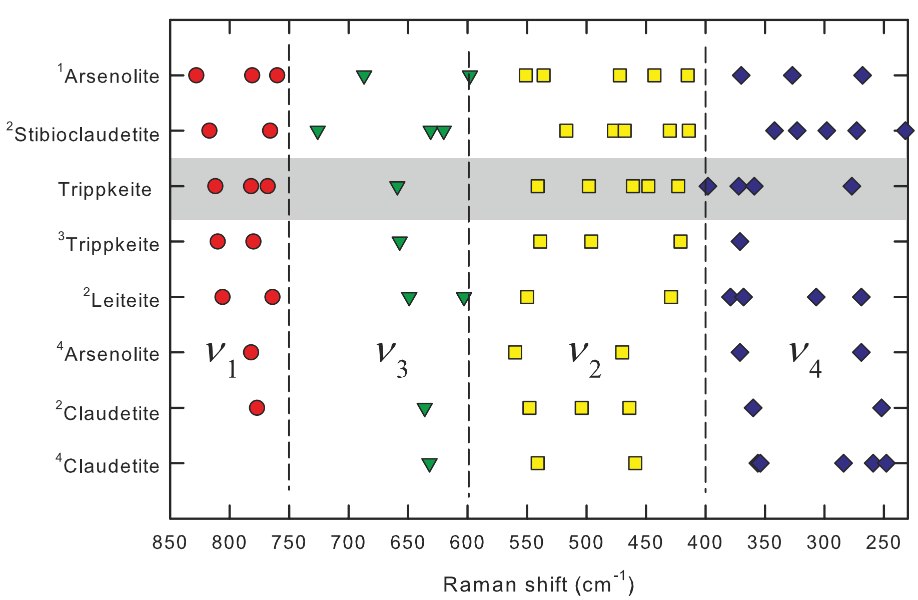

Fig. 6 Positions of the ν_1, ν_3, ν_2 and ν_4 vibrational modes in trippkeite together with minerals containing AsO_3 pyramidal group data after [1]Gilliam et al. (2003), [2]Origlieri et al. (2009), [3]Bahfenne et al. (2011), [4]Flynn et al. (1976).

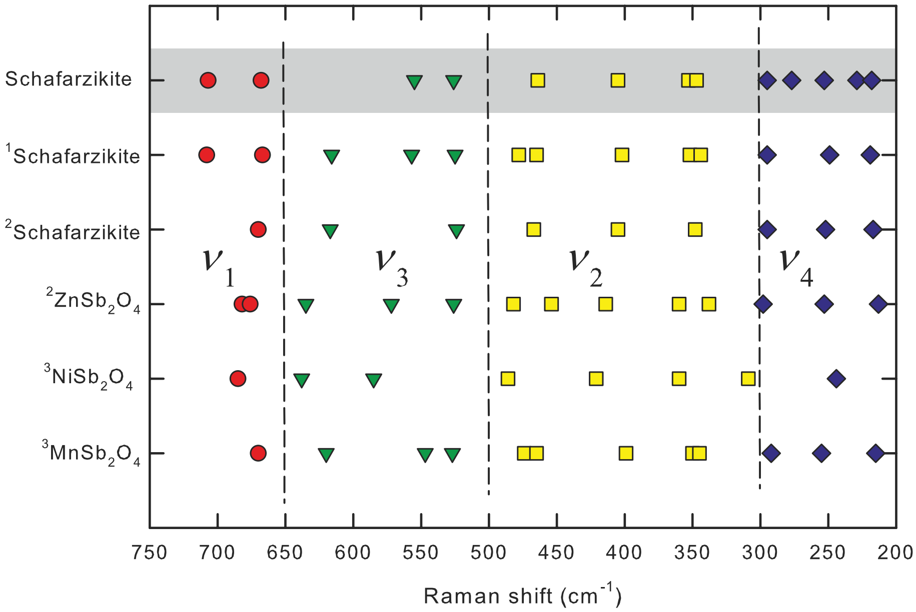

Fig. 7 Band positions in schafarzikite compared with the ν_1, ν_3, ν_2 and ν_4 vibrations in minerals containing SbO_3 pyramidal group, data after [1]Bahfenne et al. (2011), [2]Sejkora et al (2007), [3]Chater et al. (1986).

trippkeite and between 480 and 400 cm^{-1} in schafarzikite can be attributed to the vibrational modes of the $As(Sb)O_3$ rather than the frequencies arising from the stretching of the Cu(Fe)–O as suggested by Bahfenne et al. (2011). The same observations have been noticed by Kharbish et al. (2007, 2009) and Kharbish (2011) in minerals containing isolated and interconnected As(Sb) S_3 pyramidal groups. Furthermore, it can be concluded from Figs 6 and 7 that the symmetric ν_1 (A_1) As(Sb)–O stretching modes occur between 850–750 and between 750–650 cm^{-1} for trippkeite and schafarzikite, respectively. The antisymmetric As(Sb)–O stretching vibrations appear in the region between 750–600 and between 650–500 cm^{-1}, respectively (Figs 6–7). The symmetric ν_2 (A_1) O–As(Sb)–O bending modes occur in the spectral regions 600–400 and 500–300 cm^{-1}, respectively, and those for the antisymmetric ν_4 (E) modes between 400–250 and 300–200 cm^{-1} (Figs 6–7).

The above discussion reveals that no striking differences in the spectral features are evident between minerals containing isolated and interconnected $(As,Sb)O_3$ groups. The latter observation has been also noticed for isolated and interconnected $(As,Sb)S_3$ groups by Kharbish et al. (2009) and Kharbish (2011).

Acknowledgements. The author is grateful to Prof. A. Beran and Prof. E. Libowitzky, for their help during the Raman measurements. Thanks are due to Prof. F. Pertlik for kindly providing samples and Prof. H. Effenberger for carrying out unit-cell parameter measurements. In addition to useful scientific comments, handling editor Dr. J. Sejkora as well as J. Plášil and an anonymous reviewer helped to improve the quality of the English text.

References

Beattie IR, Livingston KMS, Ozin GA, Reynolds DJ (1970) Single-crystal Raman spectra of arsenolite (As_4O_6) and senarmonite (Sb_4O_6). The gas-phase Raman spectra of P_4O_6, P_4O_{10}, and As_4O_6. J Chem Soc A: 449–451

Bahfenne S (2011) Single Crystal Raman Spectroscopy of Selected Arsenite, Antimonite and Hydroxyantimonite Minerals. Unpublished Ph.D. thesis, Queensland University of Technology, pp 1–159

Bahfenne S, Rintoul L, Frost, RL (2011) Single crystal Raman spectroscopy of natural schafarzikite $FeSb_2O_4$ from Pernek, Slovak Republic. Am Mineral 96: 888–894

Brumbach SB, Rosenblatt GM (1972) In-cavity laser Raman spectroscopy of vapors at elevated temperatures. As_4 and As_4O_6. J Chem Phys 56: 3110–3118

Chater R, Gavarri JR, Genet F (1986) Composes isomorphes $MeX_2O_4E_2$: I. Etude vibrationnelle de $MnSb_2O_4$ entre 4 et 300 K: champ de force et tenseur élastique. J Solid State Chem 63: 295–307

Cotton FA, Wilkinson G (1966) Advanced Inorganic Chemistry (6th edition). John Wiley & Sons, New Jersey, pp 1–1376

Eby RK, Hawthorne FC (1993) Structural relations in copper oxysalt minerals. I. Structural hierarchy. Acta Cryst B49: 28–56

Emmerling F, Röhr C (2003) Die neuen Oxoarsenate(III) $AAsO_2$ (A = Na, K, Rb) und $Cs_3As_5O_9$. Darstellung, Kristallstrukturen und Raman-Spektren. Z Naturforsch 58: 620–626

Fischer R, Pertlik F (1975) Verfeinerung der Kristallstruktur des Schafarzikits, $FeSb_2O_4$. Tschermaks Min Petr Mitt 22: 236–241

Flynn EJ, Solin SA, Papatheodorou GN (1976) Vibrational excitations of As_2O_3. II. Crystalline phases. Phys Rev B13: 1752–1758

Ghose S, Sen Gupta PK, Schlemper EO (1987) Leiteite, $ZnAs_2O_4$: a novel type of tetrahedral layer structure with arsenite chains. Am Mineral 72: 629–632

Gilliam SJ, Merrow CN, Kirkby SJ, Jensen JO, Zeroka D, Banerjeeb A (2003) Raman spectroscopy of arsenolite: crystalline cubic As_4O_6. J Solid State Chem 173: 54–58

Grzechnik A (1999) Compressibility and vibrational modes in solid As_4O_6. J Solid State Chem 144: 416–422

Hinrichsen B, Dinnebier RE, Rajiv P, Hanfland M, Grzechnik A, Jansen M (2006) Advances in data reduction of high-pressure X-ray powder diffraction data from two-dimensional detectors: a case study of schafarzikite ($FeSb_2O_4$). J Phys Condens Mat 18/25: S1021–S1037

Hirschle C, Röhr C (2000) Alkalimetall-Oxoantimonate: Synthesen, Kristallstrukturen und Schwingungsspektren von $ASbO_2$ (A = K, Rb), $A_4Sb_2O_5$ (A = K, Rb, Cs) und Cs_3SbO_4. Z Anorg Allg Chem 626: 1305–1312

Jensen JO, Gilliam SJ, Banerjeeb A, Zeroka D, Kirkby SJ, Merrow, CN (2003) A theoretical study of As_4O_6: vibrational analysis, infrared and Raman spectra. J Mol Struct (Theochem) 664–665: 145–156

Kharbish S (2011) Raman spectroscopic investigations of some Tl-sulfosalt minerals containing pyramidal (As,Sb) S_3 groups. Am Mineral 96: 609–616

Kharbish S, Libowitzky E, Beran A (2007) The effect of As–Sb substitution in the Raman spectra of tetrahedrite–tennantite and pyrargyrite–proustite solid solutions. Eur J Mineral 19: 567–574

Kharbish S, Libowitzky E, Beran A (2009) Raman spectra of isolated and interconnected pyramidal XS_3 groups (X = Sb,Bi) in stibnite, bismuthinite, kermesite, stephanite and bournonite. Eur J Mineral 21: 325–333

Krenner JA (1921) Schafarzikite, ein neues Mineral. Z Kristallogr 56: 198–200

Lee C, Harrison WTA (2004) The catena–arsenite chain anion, $[AsO_2]^{n-}_n$: $(H_3NCH_2CH_2NH_3)_{0.5}[AsO_2]$ and $NaAsO_2$. Acta Cryst C60: m215–m218

Loehr TM, Plane RA (1968) Raman spectra and structures of arsenious acid and arsenites in aqueous solution. Inorg Chem 7: 1708–1714

Lucovsky G, Galeener FL (1980) Local structure and vibrational spectra of νAs_2O_3. J Non-Cryst Solids 37: 53–70

Mellini M, Merlino S (1979) Versiliaite and apuanite: derivative structures related to schafarzikite. Am Mineral 64: 1235–1242

Nakamoto K (1997) Infrared and Raman Spectra of Inorganic and Coordination Compounds. Part A: Theory and Applications in Inorganic Chemistry (6th edition). John Wiley & Sons, New Jersey, pp 1–419

Origlieri MJ, Downs RT, Pinch WW, Zito, GL (2009) Stibioclaudetite $AsSbO_3$. A new mineral from Tsumeb, Namibia. Mineral Rec 40: 209–213

Otwinowski Z, Minor W (1997) Processing of X-ray diffraction data collected in oscillation mode. In: Carter CW, Sweet RM (eds) Methods in Enzymology. Academic Press, New York, pp 307–326

Pertlik F (1975) Verfeinerung der Kristallstruktur von synthetischem Trippkeit, $CuAs_2O_4$. Tschermaks Min Petr Mitt 22: 221–217

Pertlik F (1988) The single chain arsenites $Pb(AsO_2)Cl$ and $Pb_2(AsO_2)_3Cl$. Preparation and structure investigation. Z Kristallogr 184: 191–201

Sejkora J, Ozdín D, Vitáloš J, Tuček P, Čejka J, Duďa R (2007) Schafarzikite from the type locality Pernek (Malé Karpaty Mountains, Slovak Republic). Eur J Mineral 19: 419–427

Wang A, Han J, Guo L, Yu J, Zeng P (1994) Database of standard Raman spectra of minerals and related inorganic crystals. Appl Spectrosc 48: 959–968

Zemann J (1951a) Formel und Kristallstruktur des Schafarzikits. Tschermaks Min Petr Mitt 2: 166–175

Zemann J (1951b) Formel und Kristallstruktur des Trippkeits. Tschermaks Min Petr Mitt 2: 417–423